QHETI: A Quadrant-Based Imaging Framework for Transfer Learning in Heterogeneous Tabular Data

Hidden for double-blind review

ABSTRACT

Personalized health risk prediction is critical for early intervention and preventive care, yet remains challenging due to limited patient-level data and high variability in clinical datasets. Tabular health records such as lab results, vital signs, and monitoring data are widely used in biomedical informatics, but their heterogeneity across institutions and populations often hinders the development of generalizable prediction models. Traditional transfer learning (TL) approaches struggle in this context due to incompatible feature spaces and small sample sizes. To address these challenges, we propose Quadrant-based Heterogeneous Tabular Imaging (QHETI), a novel deep learning framework that enables cross-domain TL for heterogeneous tabular health data. QHETI transforms tabular records into semantically organized 2D image representations by grouping related features into spatial quadrants. This design enables the use of pretrained 2D convolutional neural networks (CNNs), originally developed for image data, as feature extractors without requiring shared feature alignment between datasets. We evaluate QHETI on a personalized asthma risk prediction task using real-world patient data, where population-level models are fine-tuned and adapted to individual patients. The extracted features are used to train conventional classifiers. Results show that QHETI achieves strong predictive performance, with sensitivity ranging from 0.62 to 0.77, and outperforms a baseline CNN model. Notably, the best-performing model, TL-KNN, achieves a 13.75% improvement in sensitivity. These findings demonstrate QHETI's potential to improve health risk prediction in data-scarce and heterogeneous clinical settings.

CCS CONCEPTS

• **Computing methodologies** → **Learning paradigms**; **Machine learning algorithms**.

KEYWORDS

heterogeneous transfer learning, tabular data representation, deep feature extraction, personalized health prediction

ACM Reference Format:

Hidden for double-blind review. 2025. QHETI: A Quadrant-Based Imaging Framework for Transfer Learning in Heterogeneous Tabular Data. In *The 34th ACM International Conference on Information and Knowledge Management (CIKM'25), November 10–14, 2025, Seoul, Korea.* ACM, New York, NY, USA, 5 pages. https://doi.org/10.1145/xxxxxxx.xxxxxxx

CIKM '25, November 10–14, 2025, Seoul, Korea

ACM ISBN 979-x-xxxx-xxxx-xx/xx/xx
https://doi.org/10.1145/xxxxxxx.xxxxxxx

1 INTRODUCTION

Tabular data is a dominant format in biomedical research and health-related applications, commonly used to represent structured information such as electronic health records, lab results, and patient monitoring data. These datasets are central to predictive modeling for precision medicine. However, developing accurate individual-level risk prediction models remains challenging due to two primary limitations: (1) the small size of individual patient datasets, often limited to a few hundred observations, and (2) the heterogeneity of tabular data across institutions, populations, and clinical workflows, where feature types, semantics, and formats can vary significantly. These limitations hinder the effective use of deep learning, which typically requires large, homogeneous datasets to learn robust representations [4, 5].

While transfer learning (TL) has shown promise in other domains by enabling models to reuse knowledge from data-rich source domains [14, 32], its application to clinical tabular data remains limited. The heterogeneity of clinical datasets, characterized by misaligned feature spaces, varying distributions, and lack of shared inductive biases, pose fundamental challenges for conventional fine-tuning and domain adaptation techniques [2, 31].

To address these challenges, we propose Quadrant-based Heterogeneous Tabular Imaging (QHETI), a deep learning framework for transfer learning across heterogeneous tabular datasets. QHETI converts tabular records into structured 2D image representations by organizing semantically related features into spatial quadrants. This enables the use of pretrained 2D convolutional neural networks (CNNs), originally developed for vision tasks, as general-purpose feature extractors. By removing the requirement for aligned feature spaces, QHETI supports knowledge transfer between datasets with non-overlapping or partially overlapping features. In our asthma risk prediction, we retrain a CNN on population-level data, fine-tune it on a target patient's data with a different feature set, and use the resulting representations to train conventional classifiers for individualized prediction.

To our knowledge, this is the first approach to apply 2D CNNs as feature extractors for heterogeneous tabular data. QHETI introduces a novel imaging-based transformation that organizes feature inputs semantically, enabling pretrained CNNs to operate in highly variable clinical settings. It supports transfer learning across misaligned feature spaces and integrates seamlessly with conventional classifiers. This work offers a flexible and generalizable framework for knowledge transfer in complex tabular domains, with particular relevance for personalized risk modeling in data-scarce healthcare contexts.

2 RELATED WORK

TL has been foundational in domains like computer vision and natural language processing, where large-scale labeled datasets and shared structures support cross-domain knowledge reuse [14, 22].

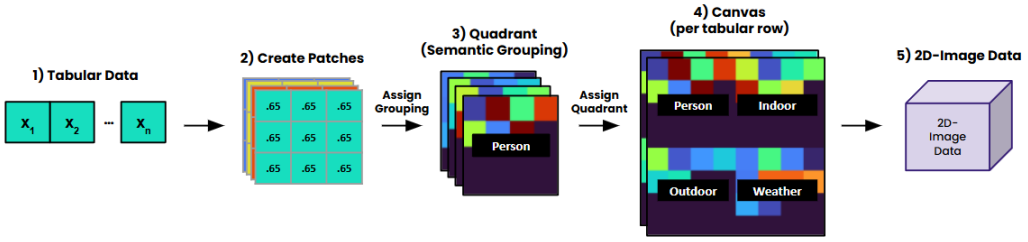

(a) Tabular to 2D image conversion

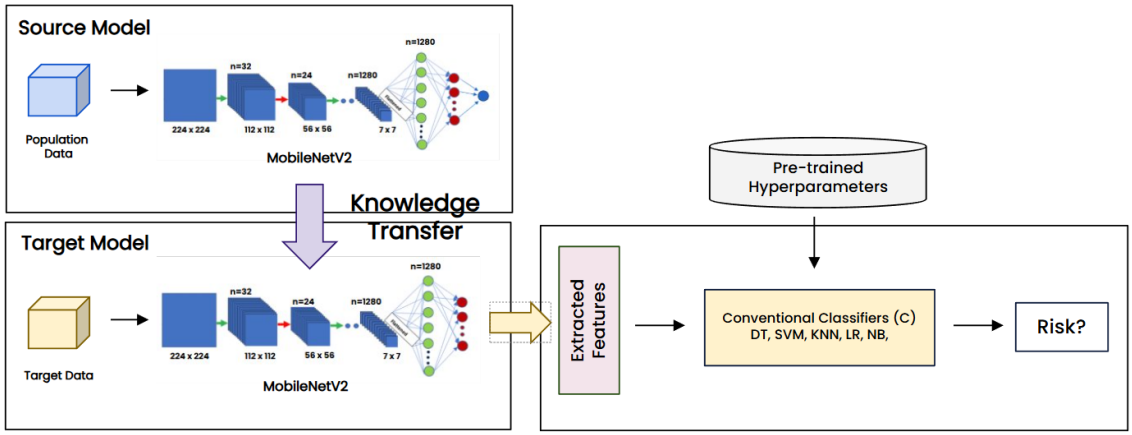

(b) TL with CNN as a feature extractor and classification

Figure 1: QHETI framework

Common strategies include instance reweighting, mapping-based adaptation, and latent-space alignment [26, 32]. A parallel line of work emphasizes pretrained models as general-purpose feature extractors, with notable success in object detection and semantic segmentation [6, 16]. However, traditional TL methods generally assume aligned feature spaces across domains. While models based on domain-invariant embedding learning [3, 9, 12, 13, 23] work well in homogeneous settings, they often fail in heterogeneous scenarios where feature sets or semantics differ significantly [5, 31].

To overcome these limitations, various strategies have been proposed for transferring knowledge across structurally divergent tabular datasets [7, 8, 20, 25]. A comprehensive survey by [2] categorizes such techniques into instance-level reweighting, shared space projection, and representation alignment. However, most rely on assumptions like latent manifold alignment or structural regularity that often fail in clinical contexts. These challenges are especially pronounced in personalized healthcare, where variability in sensors, data formats, and clinical documentation across patients introduces substantial heterogeneity [10, 29]. Recent models [21, 28] attempt to accommodate this by using domain-specific encoders or relevance-aware fine-tuning, though they remain limited to raw tabular representations and do not utilize spatial encodings.

A growing body of research has investigated transforming tabular data into 2D spatial representations to exploit the inductive biases of CNN architectures. These methods encode tabular features into image like formats using techniques based on statistical ordering, graph structures, or distance-preserving transformations [15, 19, 30]. Others have explored enhancements like synthetic spatial manipulations including rotation, duplication, and blurring, to better capture structure in unstructured data [1, 27]. More recent work has focused on making deep learning models compatible with mixed-type tabular inputs through jointly learned conversion and classification pipelines [4, 11]. While these approaches show improved performance in homogeneous settings, they generally assume consistent feature sets and do not address heterogeneous transfer learning scenarios, where semantic meaning and feature composition differ between source and target domains [18].

In our work, we build on these ideas by introducing a quadrant-based transformation framework that organizes heterogeneous features into semantically coherent spatial subgroups. This design enables pretrained models to extract transferable representations even when individual patient data vary in feature availability, supporting individual-level modeling under heterogeneous tabular conditions.

3 METHODS

3.1 QHETI Framework

Our proposed QHETI framework consists of three main parts: (1) tabular data to image conversion, (2) TL with CNN as a feature extractor, trained with population-level data and retrained with a target patient' data, and (3) new features pipelined to conventional classifiers. Figure 1 shows an overview of the tabular data to 2D

image conversion and the pipeline of CNN and the conventional classification. The process executes as follows:

(1) Convert all patients' data to 2D images.
(2) Retrain a pretrained CNN (MobileNetV2) on source data (population data) to classify each sample as class 0 (risk) or class 1 (non-risk), and save the resulting source model.
(3) Fine-tune the CNN using a target patient's data and store the target model.
(4) Remove the output layer from the target model and connect the model to a conventional classifier. Feed the classifier with the outputs of the last hidden layer of the CNN to train the classifier while freezing the CNN.

3.2 Tabular Data to Image

QHETI transforms each tabular record into a structured 2D image that spatially encodes scalar features, enabling compatibility with vision-based deep learning architectures. Each patient record is divided into four semantically meaningful feature groups, referred to as quadrants: (1) F_1: physiological/behavioral, (2) F_2: indoor air quality, (3) F_3: outdoor air quality, and (4) F_4: weather conditions. These quadrants are mapped onto distinct square regions in a unified 2×2 canvas image layout (top-left to bottom-right: F_1–F_4).

Scalar features are encoded as uniform grayscale patches, where intensity reflects the normalized feature values. The number of patches per quadrant is determined by the maximum features across all quadrants: $F_{\max} = \max(F_1, F_2, F_3, F_4)$. The grid size is then calculated, $k = \lceil \sqrt{F_{max}} \rceil$, resulting in a $k \times k$ layout per quadrant, with zero-padding applied when the number of features is less than k^2. Each quadrant occupies approximately 112×112 pixels on the image canvas, with individual patch dimensions of roughly $\lceil 112/k \rceil$ pixels. Although k may not divide evenly into 112, this layout preserves spatial structure and closely approximates the final 224×224 resolution. The resulting grayscale canvas is then color-mapped and resized to $224 \times 224 \times 3$ to match the input of the CNN [17].

3.3 Feature Extraction and Classification

3.3.1 Source modeling: Each population sample of 30 features is converted into a 2D image, organized into four quadrants. Each quadrant is mapped to a $k \times k$ grid and given the largest quadrant contains $F_{\max} = 10$ features, we compute $k = 4$. This results in a 4×4 grid per quadrant, providing 16 spatial positions to accommodate all features within the largest group (see Figure 2(a)). We adopt a MobileNetV2 (M-Net) backbone, a CNN pretrained on ImageNet, with all layers initially frozen. Then its last layer is replaced with a custom head comprising of a 'Global Average Pooling' layer, two dense layers (512, 128 units with ReLU) each followed by BN and 30% drop-out, and a sigmoid output layer. In our study, we retrain the last m layers ($m = 20$) of the source network.

3.3.2 Target modeling: Target datasets may include fewer or more features than the source. In our case, each target model is trained on 18 input features using weights transferred from the pretrained source model. These features are grouped into semantic quadrants, where again, the size determined by the largest quadrant: $F_{\max} = 7$ features. Accordingly, the grid size is set to $k = 3$, resulting in a 3×3 grid per quadrant (see Figure 2(b)). Fine-tuning is performed with varying backbone unfreezing depths ($m \in \{10, 20, 25, 30, 40\}$).

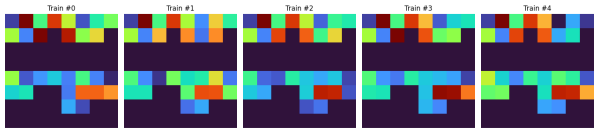

(a) Source: 30 features grouped into F_1=7, F_2=7, F_3=6, F_4=10

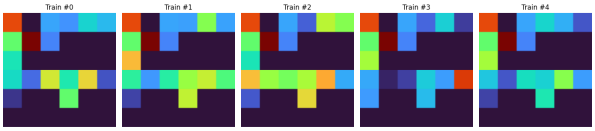

(b) Target: 18 features grouped into F_1=7, F_2=3, F_3=4, F_4=4

Figure 2: 2D image data representations

This setup introduces a domain shift due to feature mismatch while preserving structural consistency. In our study, this patient-specific model preserves population-level generalization while allowing personalized optimization.

3.3.3 Classification: In the final stage, each patient's CNN model is fine tuned and adapted through heterogeneous transfer learning, then frozen and used as a fixed feature extractor for individual level predictions. Specifically, (1) the output layer is removed and the remaining layers are frozen to preserve the transferred representations; (2) the activations from the last hidden layer, which serve as feature embeddings, are extracted; and (3) these embeddings are used to train and validate a conventional classifier.

4 EXPERIMENTS

4.1 Datasets and Experimental Design

Our dataset includes real-world data from 23 asthma patients, each with 88–210 samples and 30 features, collected in a study [double-blind]. Features include physiological measures (e.g., PEFR), behavioral attributes (e.g., house location, cooking style), and environmental exposures (e.g., indoor/outdoor air quality and weather), estimated over a 24-hour window prior to each PEFR reading. Each sample is labeled as class 0 (risk) or class 1 (non-risk), where class 0 indicates a PEFR below a patient-specific threshold, set at the 20th percentile of their own PEFR distribution.

We evaluate QHETI against a baseline CNN with all frozen layers trained only on individual patient data and used as a fixed feature extractor. Models are assessed using six standard metrics. We also compare QHETI to conventional classifiers trained directly on raw tabular data without feature extraction or transfer learning.

Each dataset is split into 80% training/validation and 20% testing. To reduce overfitting, we apply k-fold cross-validation: 5-fold for source TL models, 3-fold for target TL models, and 3-fold for conventional models, All models are trained using Adam (learning rate = 1e-4) and BCE loss. To address class imbalance, SDD-SMOTE [24] is applied to all training splits. Source models are trained in two stages: 20 epochs with all layers frozen to stabilize initial weights, followed by 100 epochs with the last m layers unfrozen for fine-tuning. Target models follow the same structure, with 100 frozen and 1,000 fine-tuning epochs using varying unfreezing depths.

Table 1: QHETI vs. Baseline CNN: classification performance gains across multiple metrics

Feature extractor	Classifier	Accuracy	Sensitivity	Specificity	Precision avg.	F_1 avg.	AUC ROC
Baseline (CNN without TL)	DT	0.6562	0.5875	0.7245	0.6425	0.6047	0.6562
	KNN	0.7117	0.6958	0.7228	0.6932	0.6484	0.7117
	LR	0.6875	0.6074	0.7673	0.6947	0.6351	0.6875
	NB	0.7019	0.6331	0.7700	0.7018	0.6534	0.7019
	SVM	0.7037	0.6376	0.7693	0.7104	0.6521	0.7037
QHETI (CNN with *TL*)	DT	0.6977 (**6.33%**)	0.6203 (**5.58%**)	0.7746 (**6.91%**)	0.6694 (**4.19%**)	0.6576 (**8.75%**)	0.6977 (**6.33%**)
	KNN	0.7991 (**12.27%**)	0.7653 (**10.00%**)	0.8323 (**15.15%**)	0.7583 (**9.39%**)	0.7552 (**16.46%**)	0.7991 (**12.27%**)
	LR	0.7768 (**12.98%**)	0.6908 (**13.75%**)	0.8625 (**12.43%**)	0.7627 (**9.79%**)	0.7503 (**18.14%**)	0.7768 (**12.98%**)
	NB	0.7869 (**12.09%**)	0.7001 (**10.59%**)	0.8733 (**13.41%**)	0.7747 (**10.38%**)	0.7635 (**16.83%**)	0.7869 (**12.09%**)
	SVM	0.7779 (**10.54%**)	0.6556 (**2.82%**)	0.8997 (**16.97%**)	0.8014 (**12.82%**)	0.7660 (**17.46%**)	0.7779 (**10.54%**)

Note: Numbers in parentheses indicate the percentage improvement compared to the baseline CNN.

Table 2: Conventional classifiers without feature extractor / no transfer learning

Classifier	Accuracy	Sensitivity	Specificity	Precision avg.	F_1 avg.	AUC ROC
DT	0.5745	0.3742	0.7747	0.5704	0.5592	0.5745
KNN	0.5967	0.5323	0.6611	0.5707	0.5522	0.5967
LR	0.6180	0.5290	0.7089	0.5894	0.5805	0.6100
NB	0.6141	0.4174	0.8109	0.6064	0.6018	0.6141
SVM	0.5659	0.3266	0.8051	0.5614	0.5578	0.5659

Table 3: Analysis of effect of unfrozen ratio in sensitivity

# unfrozen layers	*TL*-DT	*TL*-KNN	*TL*-LR	*TL*-NB	*TL*-SVM
10	0.5193	0.6478	0.5793	0.5895	0.4996
20	0.5494	0.7073	0.6151	0.6145	0.5597
25	0.5890	0.7183	0.6492	0.6505	0.6010
30	**0.6203**	**0.7653**	**0.6908**	**0.7001**	**0.6556**
40	0.6031	0.7386	0.6552	0.6627	0.6364

4.2 Experimental Results

4.2.1 QHETI vs. Baseline Models Performance Comparison. Using the optimal configuration of $m = 30$ unfrozen layers, we compare QHETI to a baseline model that uses a frozen CNN trained solely on individual patient data without population-level transfer learning. Results shown in Table 1 across five classifiers and six metrics: accuracy, sensitivity, specificity, precision average, F1-score average, and AUC ROC demonstrate consistent and substantial performance gains with QHETI. TL-KNN and TL-NB again lead in sensitivity, while TL-LR and TL-KNN show the largest improvements in F_1-score (18.14% and 10.63%) and AUC ROC (12.98% and 12.27%), respectively. These results highlight QHETI's strength in identifying high-risk cases and maintaining overall predictive balance, confirming its advantage over non-transfer models in heterogeneous, data-limited clinical settings. In addition, QHETI outperforms conventional classifiers trained directly on raw tabular data without any feature extraction or transfer learning (Table 2), demonstrating the critical role of deep feature extraction in improving predictive performance across all evaluation metrics.

4.2.2 QHETI Performance with Varying Unfrozen Layers. We analyze the effect of different transfer learning configurations by varying the number of unfrozen CNN layers from 10 to 40. Sensitivity results across five conventional classifiers show a general improvement as more layers are unfrozen, with performance peaking at 30 layers for most models. TL-KNN and TL-NB achieve the highest sensitivity at this configuration, scoring 0.7653 and 0.7001, respectively. These findings suggest that selectively fine-tuning part of the network (rather than freezing too few or too many layers) enhances the transferability of learned features for individualized health risk prediction.

5 CONCLUSION

In this paper, we introduced QHETI, a deep learning framework for transfer learning across heterogeneous tabular datasets, addressing challenges such as disjoint feature spaces and structural inconsistencies. QHETI transforms tabular records into semantically organized 2D images, enabling pretrained CNNs to act as general-purpose feature extractors. This imaging-based encoding improves predictive performance across conventional classifiers and consistently outperforms baselines, even without aligned features. Future work will extend QHETI to more complex scenarios, including testing on larger cohorts with varied feature composition, semantic sparsity, and quadrant-level dropout. We also aim to evaluate QHETI under minimal feature overlap and disrupted alignment, simulating missing modalities and domain-specific gaps to enhance its robustness and generalizability.

6 GENERATIVE AI USAGE DISCLOSURE

In accordance with the ACM CIKM 2025 policy on Generative AI (GenAI) usage disclosure and the ACM Authorship Policy, we hereby report all uses of GenAI tools in this work. No GenAI methods or outputs were employed in any aspect of modeling, data collection, data preprocessing, or algorithm design. Generative AI was used solely to assist with manuscript preparation—specifically, to identify and correct grammatical errors, typos, and spelling mistakes in the text. All substantive technical contributions, experimental design, analysis, and interpretation of results were produced entirely by the authors. This disclosure, together with the references, does not count toward the page limit.

REFERENCES

[1] Haneen A. Alenizy and Jamal Berri. 2023. Transforming tabular data into images via enhanced spatial relationships for CNN processing. *Scientific Reports* 13 (2023), 4785.

[2] Yiqing Bao, Xiaokang Ma, Zhi Zhang, and Maoguo Gong. 2022. Heterogeneous transfer learning: A survey. *Comput. Surveys* 55, 3 (2022), Article 59. https://doi.org/10.1145/3507910

[3] John Blitzer, Ryan McDonald, and Fernando Pereira. 2006. Domain adaptation with structural correspondence learning. In *Proceedings of the 2006 conference on empirical methods in natural language processing*. 120–128.

[4] Vadim Borisov, Kay Broelemann, and Gjergji Kasneci. 2023. DeepTLF: Robust deep neural networks for heterogeneous tabular data. *International Journal of Data Science and Analytics* 16 (2023), 85–100.

[5] Vadim Borisov, Tobias Leemann, Kathrin Seßler, Johannes Haug, Martin Pawelczyk, and Gjergji Kasneci. 2022. Deep neural networks and tabular data: A survey. *IEEE transactions on neural networks and learning systems* (2022).

[6] Liang-Chieh Chen, Yukun Zhu, George Papandreou, Florian Schroff, and Hartwig Adam. 2018. Encoder-decoder with atrous separable convolution for semantic image segmentation. In *Proceedings of the European conference on computer vision (ECCV)*. 801–818.

[7] Jihun Ham, Daniel D Lee, and Lawrence K Saul. 2005. Semisupervised alignment of manifolds. In *Proceedings of the 10th International Workshop on Artificial Intelligence and Statistics (AISTATS)*. 120–127.

[8] Hao Li, Sinno Jialin Pan, Shiqiang Wang, and Alex C. Kot. 2025. Heterogeneous domain adaptation via nonlinear matrix factorization. *IEEE Transactions on Neural Networks and Learning Systems* (2025). To appear.

[9] Mingsheng Long, Jianmin Wang, Guiguang Ding, Jiaguang Sun, and Philip S. Yu. 2014. Transfer joint matching for unsupervised domain adaptation. In *Proceedings of the IEEE Conference on Computer Vision and Pattern Recognition (CVPR)*. IEEE, 1410–1417. https://doi.org/10.1109/CVPR.2014.183

[10] Yao Luo, Yifan Chen, Azmain Salekin, and Tanvir Rahman. 2023. Toward foundation model for multivariate wearable sensing of physiological signals. In *Proceedings of the ACM International Joint Conference on Pervasive and Ubiquitous Computing (UbiComp '23)*. ACM.

[11] Takashi Matsuda, Keigo Uchida, and Shingo Shirakawa. 2024. HACNet: End-to-end learning of interpretable table-to-image converter and convolutional neural network. *Knowledge-Based Systems* 284 (2024), 111293.

[12] Sinno Jialin Pan, James T Kwok, Qiang Yang, et al. 2008. Transfer learning via dimensionality reduction.. In *AAAI*, Vol. 8. 677–682.

[13] Sinno Jialin Pan, Ivor W Tsang, James T Kwok, and Qiang Yang. 2010. Domain adaptation via transfer component analysis. *IEEE transactions on neural networks* 22, 2 (2010), 199–210.

[14] Sinno Jialin Pan and Qiang Yang. 2010. A Survey on Transfer Learning. *IEEE Transactions on Knowledge and Data Engineering* 22, 10 (2010), 1345–1359. https://doi.org/10.1109/TKDE.2009.191

[15] Bogdan Popovici, Vanessa Lopez, and Concha Martínez. 2020. REFINED: Feature-aware image encoding for deep learning. In *Proceedings of the European Conference on Machine Learning and Principles and Practice of Knowledge Discovery in Databases (ECML PKDD)*. Springer, 411–426.

[16] Joseph Redmon, Santosh Divvala, Ross Girshick, and Ali Farhadi. 2016. You only look once: Unified, real-time object detection. In *Proceedings of the IEEE conference on computer vision and pattern recognition*. 779–788.

[17] Mark Sandler, Andrew Howard, Menglong Zhu, Andrey Zhmoginov, and Liang-Chieh Chen. 2018. MobileNetV2: Inverted Residuals and Linear Bottlenecks. In *Proceedings of the IEEE/CVF Conference on Computer Vision and Pattern Recognition (CVPR)*. 4510–4520.

[18] Abhishek Sharma and Dinesh Kumar. 2022. Classification with 2-D convolutional neural networks for breast cancer diagnosis. *Scientific Reports* 12 (2022), 21857.

[19] Sandeep Sharma, Darryl Dillon, and Manohar Kulkarni. 2019. DeepInsight: A visual feature transformation for tabular data. In *Proceedings of the IEEE International Conference on Data Mining Workshops (ICDMW)*. IEEE, 1394–1403.

[20] Xiaoyong Shi, Qiang Liu, Wei Fan, Philip S. Yu, and Rui Zhu. 2010. Transfer learning on heterogeneous feature spaces via spectral transformation. In *Proceedings of the IEEE International Conference on Data Mining (ICDM)*. IEEE, 1049–1054. https://doi.org/10.1109/ICDM.2010.34

[21] Xiaoxiao Shu, Guo-Jun Qi, Jiliang Tang, and Jingdong Wang. 2015. Weakly-shared deep transfer networks for heterogeneous-domain knowledge propagation. In *Proceedings of the ACM International Conference on Multimedia (MM)*. ACM, 35–44.

[22] Lisa Torrey and Jude Shavlik. 2010. Transfer learning. In *Handbook of research on machine learning applications and trends: algorithms, methods, and techniques*. IGI Global, 242–264.

[23] Eric Tzeng, Judy Hoffman, Kate Saenko, and Trevor Darrell. 2017. Adversarial discriminative domain adaptation. In *Proceedings of the IEEE Conference on Computer Vision and Pattern Recognition (CVPR)*. IEEE, 7167–7176. https://doi.org/10.1109/CVPR.2017.755

[24] Qikang Wan, Xiongshi Deng, Min Li, and Haotian Yang. 2022. SDDSMOTE: Synthetic Minority Oversampling Technique based on Sample Density Distribution for Enhanced Classification on Imbalanced Microarray Data. In *The 6th International Conf. on Compute and Data Analysis*. 35–42.

[25] Chang Wang and Sridhar Mahadevan. 2011. Heterogeneous domain adaptation using manifold alignment. In *Proceedings of the International Joint Conference on Artificial Intelligence (IJCAI)*. AAAI Press, 1541–1546.

[26] Karl Weiss, Taghi M Khoshgoftaar, and DingDing Wang. 2016. A survey of transfer learning. *Journal of Big data* 3 (2016), 1–40.

[27] Kazuhiro Yamamoto and Shota Murata. 2022. TINTO: Tabular data to image using topology-preserving transformations. In *Proceedings of the Thirty-Sixth Conference on Neural Information Processing Systems (NeurIPS)*.

[28] Dapeng Yang, Xiaodan Peng, Xiaoyu Wu, Hao Huang, and Wei Zhong. 2025. Domain perceptive-pruning and fine-tuning for heterogeneous transfer learning in cross-domain prediction. *Expert Systems with Applications* 234 (2025), 120581.

[29] Hong Yang, Jia Li, Ming Hao, Wei Zhang, Haibo He, and Arun Kumar Sangaiah. 2024. An efficient personalized federated learning approach in heterogeneous environments: A reinforcement learning perspective. *Scientific Reports* 14, 1 (2024), 28877.

[30] Cheng Zhang, Yang Song, and Wei Zhang. 2023. IGTD: Image generation from tabular data via distance-preserving transformations. In *Proceedings of the AAAI Conference on Artificial Intelligence (AAAI)*. AAAI Press, 16092–16100.

[31] Yuchen Zhu, Yifan Chen, Zhengdong Lu, Sinno Jialin Pan, Gui-Rong Xue, Yong Yu, and Qiang Yang. 2011. Heterogeneous transfer learning for image classification. In *Proceedings of the AAAI Conference on Artificial Intelligence (AAAI)*. AAAI Press, 1304–1309.

[32] Fuzhen Zhuang, Zhiyuan Qi, Keyu Duan, Dongbo Xi, Yongchun Zhu, Hengshu Zhu, Hui Xiong, and Qing He. 2020. A comprehensive survey on transfer learning. *Proc. IEEE* 109, 1 (2020), 43–76.